Comparison of NGA-West2 GMPEs

Nick Gregor,[a] M.EERI, **Norman A. Abrahamson,[b]** M.EERI,
Gail M. Atkinson,[c] M.EERI, **David M. Boore,[d] Yousef Bozorgnia,[e]** M.EERI,
Kenneth W. Campbell,[f] M.EERI, **Brian S.-J. Chiou,[g]**
I. M. Idriss,[h] Hon.M.EERI, **Ronnie Kamai,[i]** M.EERI, **Emel Seyhan,[j]** M.EERI,
Walter Silva,[k] M.EERI, **Jonathan P. Stewart,[j]** M.EERI, **and**
Robert Youngs,[l] M.EERI

A presentation of the model parameters and comparison of the median ground-motion values from the NGA-West2 GMPEs is presented for a suite of deterministic cases. In general, the median ground motions are similar, within a factor of about 1.5–2.0 for $5 < \mathbf{M} < 7$ and distances between 10–100 km. Differences increase (on the order of 2–3) for large-magnitude ($\mathbf{M} > 8$) earthquakes at large distances ($R > 100-200$ km) and for close distances ($R < 10$ km). A similar increase is observed for hanging-wall sites, and slightly larger differences are observed for soil sites as opposed to rock sites. Regionalization of four of the GMPEs yields similar attenuation rate adjustments based on the different regional data sets. All five GMPE aleatory variability models are a function of magnitude with higher overall standard deviations values for the smaller magnitudes when compared to the large-magnitude events. [DOI: 10.1193/070113EQS186M]

INTRODUCTION

Following the same successful approach (Powers et al. 2008) that was used for the development of the original NGA-West1 ground motion prediction equations (GMPEs), five developer teams were tasked with developing updated GMPEs for estimating ground motions and aleatory variability from shallow crustal earthquakes in active tectonic regions (Bozorgnia et al. 2014). These new GMPEs are based on the significantly expanded NGA-West2 database (Ancheta et al. 2014). During the development of these new GMPEs, the developer teams held many workshop meetings in which technical results and specifics with regard to the strengths and weaknesses of individual models were

[a] Bechtel Corporation, San Francisco, CA
[b] PG&E, San Francisco, CA
[c] University of Western Ontario, London, Ontario, Canada
[d] U.S. Geological Survey, Menlo Park, CA
[e] PEER, UC Berkeley, Berkeley, CA
[f] Core Logic EQECAT, Oakland, CA
[g] California Department of Transportation, Sacramento, CA
[h] University of California, Davis, CA
[i] PEER, University of California Berkeley, CA
[j] University of California, Los Angeles, CA
[k] Pacific Engineering and Analysis, El Cerrito, CA
[l] AMEC E&I, Oakland, CA

presented and discussed. The objective of this paper is to present several comparisons between the five GMPEs and, when applicable, discuss the similarities and differences between the models in a manner similar to that of Abrahamson et al. (2008) for the original NGA-West1 GMPEs. The technical analysis and support for the development of the individual GMPEs can be reviewed in the accompanying papers in this special volume: Abrahamson et al. (ASK; 2014), Boore et al. (BSSA; 2014), Campbell and Bozorgnia (CB; 2014), Chiou and Youngs (CY; 2014), and Idriss (IM; 2014). Although several comparison cases are presented in this paper, it does not represent a complete and exhaustive set of comparisons between the models for specific cases, and as such, the general conclusions of the comparisons may not directly apply to some engineering applications.

DATA SET SELECTION AND MODEL APPLICABILITY RANGE

The NGA-West2 database has been significantly expanded relative to both the number of ground-motion recordings and associated metadata (Ancheta et al. 2014). This new database consists of 21,336 three-component recordings from 600 shallow crustal earthquakes, with a large percentage of the increase in data from small-to-moderate events within the magnitude range of **M** 3–5.5. As part of the NGA-West2 database, a new classification scheme of Class 1 and Class 2 events, as defined and presented in Wooddell and Abrahamson (2014), is provided in the flatfile. Each developer team was provided the NGA-West2 database and allowed to select the data used for their analysis. These selection criteria are presented in the accompanying papers for each specific GMPE. BSSA and CB defined Class 2 events as events within centroid R_{JB} distances of less than 10 km. CY defined the R_{JB} distance as 20 km. The ASK team only excluded Class 2 events from the Wenchuan earthquake sequence based on the observation that those motions have different spectral shapes. The BSSA team concluded that there was no observable bias between the Class 1 and Class 2 ground motions and hence did not exclude Class 2 events. For the IM model, all Class 2 events were considered, but a more restrictive magnitude range of 4.5–7.9 was applied to the NGA-West2 database. In general, four models—ASK, BSSA, CB, and CY—used more than 12,000 recordings from more than 300 earthquakes for their analysis, while the IM model consisted of more than 7,000 recordings from 160 earthquakes.

Based on the final selected data sets used for each of the five GMPEs and the specifics of the individual models, the applicable ranges, in terms of magnitude, distance, V_{S30} values, and spectral periods, are listed in Table 1. Additional application range constraints

Table 1. Model applicability range of the five GMPEs for magnitude, distance, V_{S30}, and spectral period

	ASK	BSSA	CB	CY	IM
Magnitude (mechanism)	3.0–8.5 (All)	3.0–8.5 (SS, RV) 3.3–7.0 (NM)	3.3–8.5 (SS) 3.3–8.0 (RV) 3.3–7.0 (NM)	3.5–8.5 (SS) 3.5–8.0 (RV, NM)	5.0–8.0 (All)
Distance (km)	0–300	0–400	0–300	0–300	0–150
V_{S30} (m/s)	180–1,500	150–1,500	150–1,500	180–1,500	450–2,000
Period range	PGA–10 s, PGV	PGA–10 s, PGV	PGA–10 s, PGV	PGA–10 s	PGA–10 s

(e.g., depth to 1.0 km/s boundary) not listed in Table 1 are identified in the individual GMPE papers.

MODEL FUNCTIONAL FORMS

Each of the five GMPEs incorporates saturation as a function of magnitude at short distances for short-period ground motions. Recently, it has been observed that the original NGA-West1 GMPEs leads to an overprediction of ground motions from small-to-moderate earthquakes (Chiou et al. 2010, Atkinson and Boore 2011, Campbell 2011). Based on the expanded NGA-West2 database, four of the five GMPEs (ASK, BSSA, CB, and CY) now contain a change in the magnitude scaling to account for this overprediction for small-to-moderate-magnitude events. Since the IM model is constrained for events of $\mathbf{M} \geq 5$ events this change in magnitude scaling was not part of the model.

Each of the five models contains a style of faulting factor that is based on their respective focal mechanism classifications. This dependency decreases with magnitude; ASK, CB, and CY models reduce this factor to zero for $\mathbf{M} \leq 4.0-4.5$. The BSSA and IM models have a style of faulting factors that are $\mathbf{M}$-independent. Three models (ASK, CB, and CY) contain explicit functional forms for hanging-wall sites and a rupture depth term. The BSSA model implicitly accounts for hanging-wall features through the use of the Joyner-Boore distance and did not incorporate a rupture depth term, because they found that this effect was not significant for $\mathbf{M} > 5$ earthquakes. The rupture depth term for the CB model is hypocentral depth, which is correlated with the style of faulting factor. The IM model does not include function forms for these features.

All five GMPEs are defined for a range in V_{S30} values (see Table 1). The NGA-West2 database contains a large increase in the amount of data and associated metadata (Seyhan et al. 2014) that was used to partially derive empirical site response terms in each of the five GMPEs. Numerical simulations of nonlinear site amplification factors by Kamai et al. (2014) were used for constraining the site component of site response in the ASK model, whereas CB retained the results of prior nonlinear simulations by Walling et al. (2008). Seyhan and Stewart (2014) derived a semi-empirical nonlinear site response model used by BSSA based on empirical data analysis and on the Kamai et al. (2014) simulations. CY used nonlinear site terms derived solely from data analysis. The IM model contains a linear site amplification feature based on the more restrictive V_{S30} range. The nonlinear site amplification factor is a function of the either the PGA (BSSA and CB) for a reference site condition or the pseudo-spectral acceleration (ASK and CY) for a reference site condition. The ASK, BSSA, and CY models also incorporate a factor that is dependent on the depth to the 1.0 km/s shear wave boundary ($Z_{1.0}$), and the CB model uses the depth to the 2.5 km/s shear wave boundary ($Z_{2.5}$). These additional factors are needed to better characterize basin effects that are not fully modeled with a V_{S30} value and functional model. Based on the NGA-West2 database new region specific empirical relationships are provided for these depth-to-boundary values as a function of V_{S30} for use with their GMPEs.

Based on the significant increase in non-California ground-motion data in the NGA-West2 database, four of the GMPEs have developed regional adjustments for either site response (ASK, BSSA, CB, and CY) and/or the long-distance anelastic attenuation between various geographical regions (ASK, CB, and CY). BSSA incorporated only the regional

attenuation adjustment feature in their model. The separate regions considered were Taiwan (ASK), Taiwan and California (BSSA), eastern China (ASK, CB), Japan (ASK, CB), China and Turkey (BSSA), Italy and Japan (BSSA, CY), and Wenchuan (CY). For the CY model, the Italy and Japan adjustments are only applicable for magnitudes between 6–6.9, and for the Wenchuan adjustments, only for that specific earthquake.

All five GMPE aleatory variability models are defined as a function of **M**. The four models that have nonlinear site response (ASK, BSSA, CB, and CY) include an aleatory variability model with the site amplification effects incorporated into the model.

MODEL PARAMETERS

A summary of the model parameters for the five GMPEs is given in Table 2. In general, the individual parameterization for each GMPE is similar in complexity to the original NGA-West1 GMPEs and recommended guidance for certain parameters based on empirical data are provided in the specific references for each GMPE model. Several of these parameters, as noted, are included only as part of the hanging-wall model. Style of faulting terms are defined for all five models for strike-slip and reverse events, and are defined for normal events for the ASK, BSSA, CB, and CY models. An additional classification for unspecified style of faulting is parameterized for the BSSA model. Only the ASK model is defined separately for Class 2 events. The BSSA model is considered applicable for both Class 1 and Class 2 events.

The primary distance metric for the ASK, CB, CY, and IM models is the closest distance to the rupture plane, R_{RUP}. The BSSA model uses the closest distance to the horizontal projection of the rupture plane, R_{JB}. This distance metric is also used by the ASK, CB, and CY for their hanging-wall functional model. The three models that directly model a hanging-wall effect (ASK, CB, and CY) use the R_X distance in their functional models, and the ASK model introduces a new distance metric, R_{Y0}, for their hanging-wall model but provide an alternative version that does not require knowledge of this new parameter. In addition to the depth to the top of rupture (Z_{TOR}) being used in three of the models (ASK, CB, and CY), the depth of the hypocenter, Z_{HYP}, was included in the CB model as a general earthquake depth term and is applied for all cases, whereas Z_{TOR} is used only in their hanging-wall model. BSSA found neither depth parameter to be necessary for ground-motion prediction with their functional model.

For the site response terms, all five models use the average shear-wave velocity in the top 30 m, V_{S30}, as the primary site parameter. In addition, ASK, BSSA, and CY use the $Z_{1.0}$, and CB uses the $Z_{2.5}$ boundary values. These additional model parameters listed in Table 2 and described in the specific individual references for each GMPE are included to try to capture the observed difference in site amplification from stations located in sedimentary basins. For the nonlinear site response factors, the ASK, BSSA, CB, and CY models use either the PGA or pseudo-spectral acceleration (PSA) for the spectral period of interest at different reference site conditions (i.e., either a V_{S30} value of 760 m/s or approximately 1,100 m/s) as listed in Table 2.

MEDIAN VALUE COMPARISONS

In comparing median values from the five GMPEs, several input parameters must be estimated based on each given event scenario for the fault geometry and site amplification

Table 2. Summary of model parameters used in the five GMPEs

Parameter	ASK	BSSA	CB	CY	IM
Moment magnitude	**M**	**M**	**M**	**M**	**M**
Depth to top of tupture (km)	Z_{TOR}, Z_{TOR}^b	–	Z_{TOR}^b	$Z_{TOR}Z_{TOR}^b$	–
Hypocentral depth (km)	–	–	Z_{HYP}	–	–
Style of faulting[a]	SS, RV, NM	SS, RV, NM, U	SS, RV, NM	SS, RV, NM	SS, RV
Class 2 event flag	F_{AS}	–	–	–	–
Dip (degrees)	δ^b	–	δ, δ^b	δ, δ^b	–
Down-dip rupture width (km)	W^b	–	W^b	–	–
Closest distance to rupture plane (km)	R_{RUP}	–	R_{RUP}	R_{RUP}	R_{RUP}
Horizontal distance to surface project of rupture plane (km)	R_{JB}^b	R_{JB}	R_{JB}^b	R_{JB}^b	–
Horizontal distance to top edge of rupture plane measured perpendicular to strike (km)	R_X^b	–	R_X^b	R_X^b	–
Horizontal distance off the end of rupture plane measured parallel to strike (km)	R_{Y0}^b	–	–	–	–
Average shear-wave velocity in top 30 m (m/s)	V_{S30}	V_{S30}	V_{S30}	V_{S30}	V_{S30}
Depth to 1.0 km/s boundary (km)	$Z_{1.0}$	$\delta Z_{1.0}$	–	$Z_{1.0}, \Delta Z_{1.0}$	–
Depth to 2.5 km/s boundary (km)	–	–	$Z_{2.5}$	–	–
Rock motion PGA for nonlinear site response	–	PGA_r	A_{1100}	–	–
Rock motion PSA for nonlinear site response	PSA_{1100}	–	–	$Y_{ref}(T)$	–
V_{S30} of rock motion used for nonlinear site response (m/s)	1,100	760	1,100	1,130	–
Regional adjustments	Taiwan, China, Japan	China/ Turkey, Italy/ Japan	E. China, Italy/ Japan	Italy/ Japan, Wenchuan	–

[a]Style of faulting terms: SS = strike-slip, RV = reverse, NM = normal, U = unspecified.
[b]Used only in hanging-wall model.

parameters. As an example, the depth to the top of rupture is required but must also be consistent with the hypocentral depth needed for the CB model. Based on the NGA-West2 data set, empirically based relationships have been developed for several parameters for use with the specific GMPEs. These specific input parameter values will be presented for each comparison case.

DISTANCE SCALING

The median attenuation of PGA for horizontal motions for a vertical dipping strike-slip earthquake from the five GMPEs is shown in Figure 1 plotted as a function of R_{JB} distance. These results are for a $V_{S30} = 760$ m/s, and the $Z_{1.0}$ and $Z_{2.5}$ values are based on the
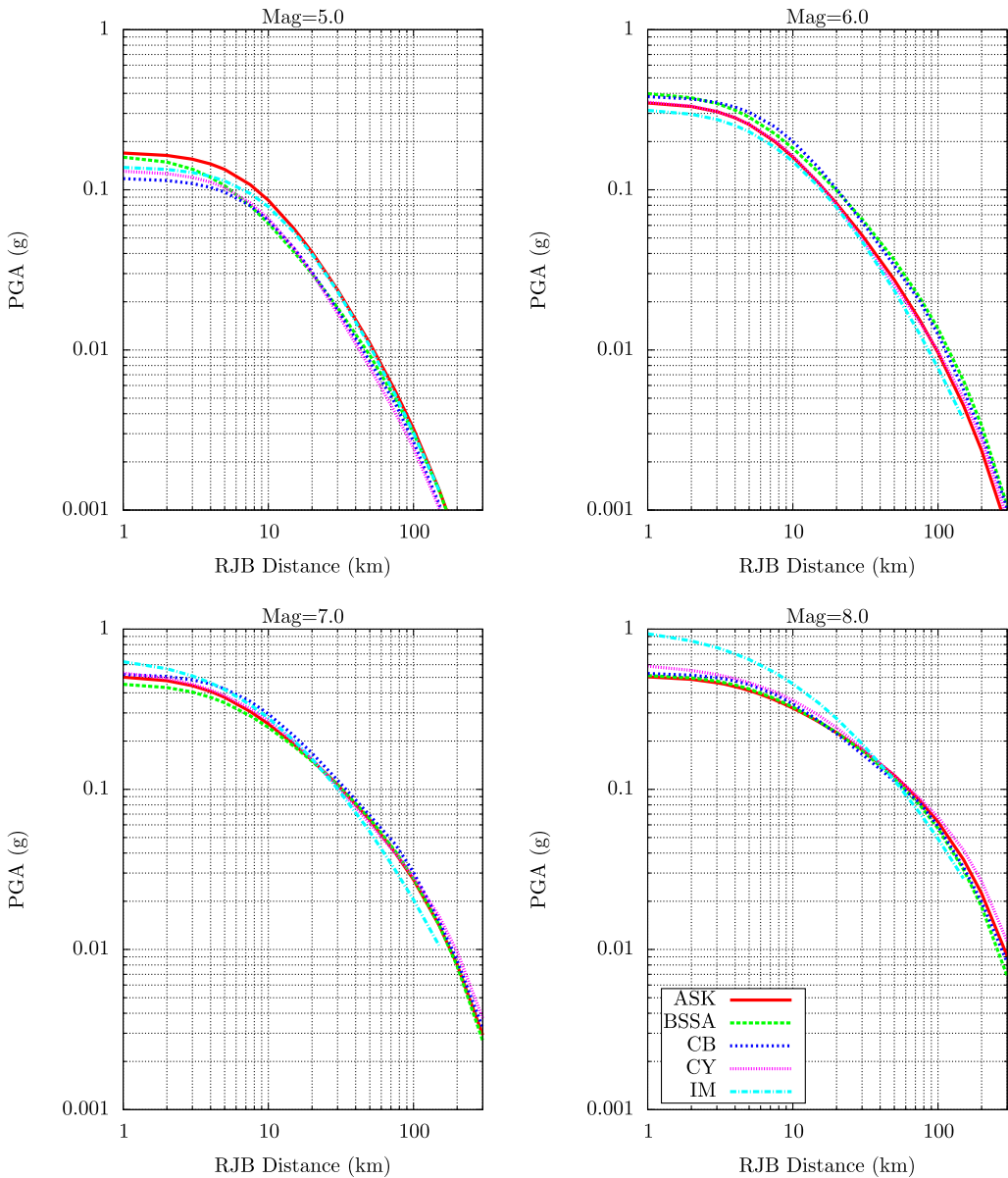
Figure 1. Comparison of distance scaling of PGA for strike-slip earthquakes for $V_{S30} = 760$ m/s.

recommended default values given for each GMPE (ASK $Z_{1.0} = 0.0481$ km, CY $Z_{1.0} = 0.0413$ km, and CB $Z_{2.5} = 0.6068$ km). For the BSSA model, the δz_1 was assigned to be 0 and for the CY the $\Delta Z1$ was set equal to 0. The depth to the top of rupture was magnitude-dependent: **M5** $Z_{TOR} = 6$ km, **M6** $Z_{TOR} = 3$ km, **M7** $Z_{TOR} = 1$ km, and **M8** $Z_{TOR} = 0$ km, and the hypocenter was placed at 8 km depth for all four magnitude values.

These results show the saturation of ground motion with decreasing distance. The five GMPEs predict similar (i.e., within a factor of 1.5) median ground motions for **M**5, 6, and 7 over the large-distance range shown in the plots. For the **M**8 results, the differences can be a factor of 2 or greater at short distances for PGA.

The same comparison plots for $T = 1.0$ s PSA are shown in Figure 2 for a $V_{S30} = 270$ m/s using the default $Z_{1.0}$ and $Z_{2.5}$ values (ASK $Z_{1.0} = 0.4704$ km,
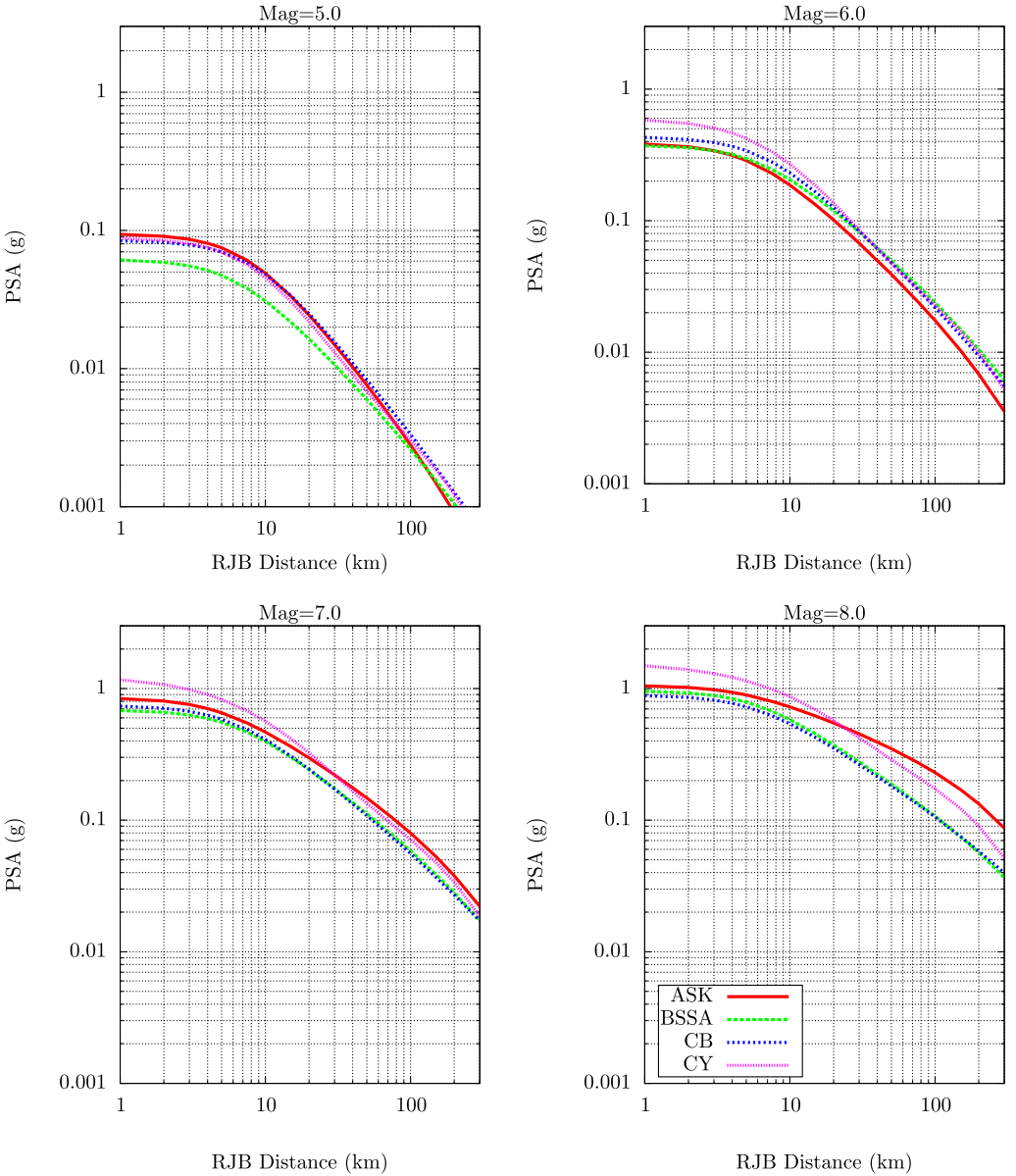
Figure 2. Comparison of distance scaling of $T = 1.0$ s PSA for strike-slip earthquakes for $V_{S30} = 270$ m/s.

CY $Z_{1.0} = 0.4794$ km and CB $Z_{2.5} = 1.9826$ km). Note that the IM model is not applicable for a V_{S30} of less than 450 m/s and is not included in these comparisons. The overall comparisons and conclusions between the models are similar to the results shown in Figure 1 for PGA, with the additional conclusion that for the **M**8 results, the differences are observed at both short and long distances.

MAGNITUDE SCALING

The effect of magnitude scaling for vertical strike-slip events at a R_{RUP} distance of 30 km is shown in Figure 3 for $V_{S30} = 760$ m/s. Plots are provided for PGA and PSA at spectral $T = 0.2$ s, 1.0 s, and 3.0 s. The **M**-dependence of the depth to top of rupture was taken based on the recommended CY model and the R_{JB} computed based on the fixed R_{RUP} distance of 30 km. The hypocenter was taken at half of the fault width assuming a square rupture area (based on a $\mathrm{Log}_{10}(\mathrm{Area}) = \mathbf{M} - 4$ relationship) down from the top of rupture for all events with a maximum seismogenic depth of 15 km for the larger events. For events with $\mathbf{M} \geq 7$, the hypocenter was fixed at a depth of 12 km. The magnitude scaling between the five models is very similar over the wide range of magnitudes.

V_{S30} SCALING

All five GMPEs are defined as a function of V_{S30}. The IM model is limited to $V_{S30} \geq$ 450 m/s and does not contain a nonlinear site amplification term. A comparison of median ground motions as a function of V_{S30} values is shown in Figures 4 and 5 for a **M**7 vertical strike-slip earthquake at $R_{JB} = 100$ and 10 km, respectively. The top of rupture was assigned to be 1 km with a hypocentral depth of 8 km. The default $Z_{1.0}$ and $Z_{2.5}$ values were used based on the empirical relationships provided for each GMPE. For the 100 km results (Figure 4), the site amplification is nearly linear, which is evident in the figures by linear variations of site amplification with V_{S30}. For higher V_{S30} values, all of the models except for CB saturate predicting constant ground motion values for higher V_{S30} values. For the shorter-distance 10 km case (Figure 5), the nonlinear effects are evident by the observed curvature in the amplification functions for ASK, BSSA, CB, and CY (downward from the linear trends in Figure 4), especially for PSA at $T = 0.2$ s. All of the models but CB have a V_{S30} value beyond which no additional amplification from nonlinearity occurs. The CB model has a V_{S30} limit of 1,500 m/s beyond which it should not be used based on the lack of a saturation floor limit in the ground motion amplification. Overall, the site amplification results are similar between the five models, especially in the range in which there is a large amount of empirical data.

HANGING WALL SCALING

A comparison of the five models showing the effects of hanging-wall scaling is shown in Figure 6 for a **M**6.7 earthquake with a dip angle of 45 degrees with a down-dip fault width of 21.97 km. The results on the left are for a surface rupture while the plots on the right are for a buried rupture at a depth of 6 km. The cross section of the two fault planes is shown in the lower parts of the figure. The attenuation curves are for PGA with a $V_{S30} = 760$ m/s and are plotted as a function of R_X distance with negative values being located on the footwall and positive values on the hanging wall. Results are shown for both normal (top) and reverse
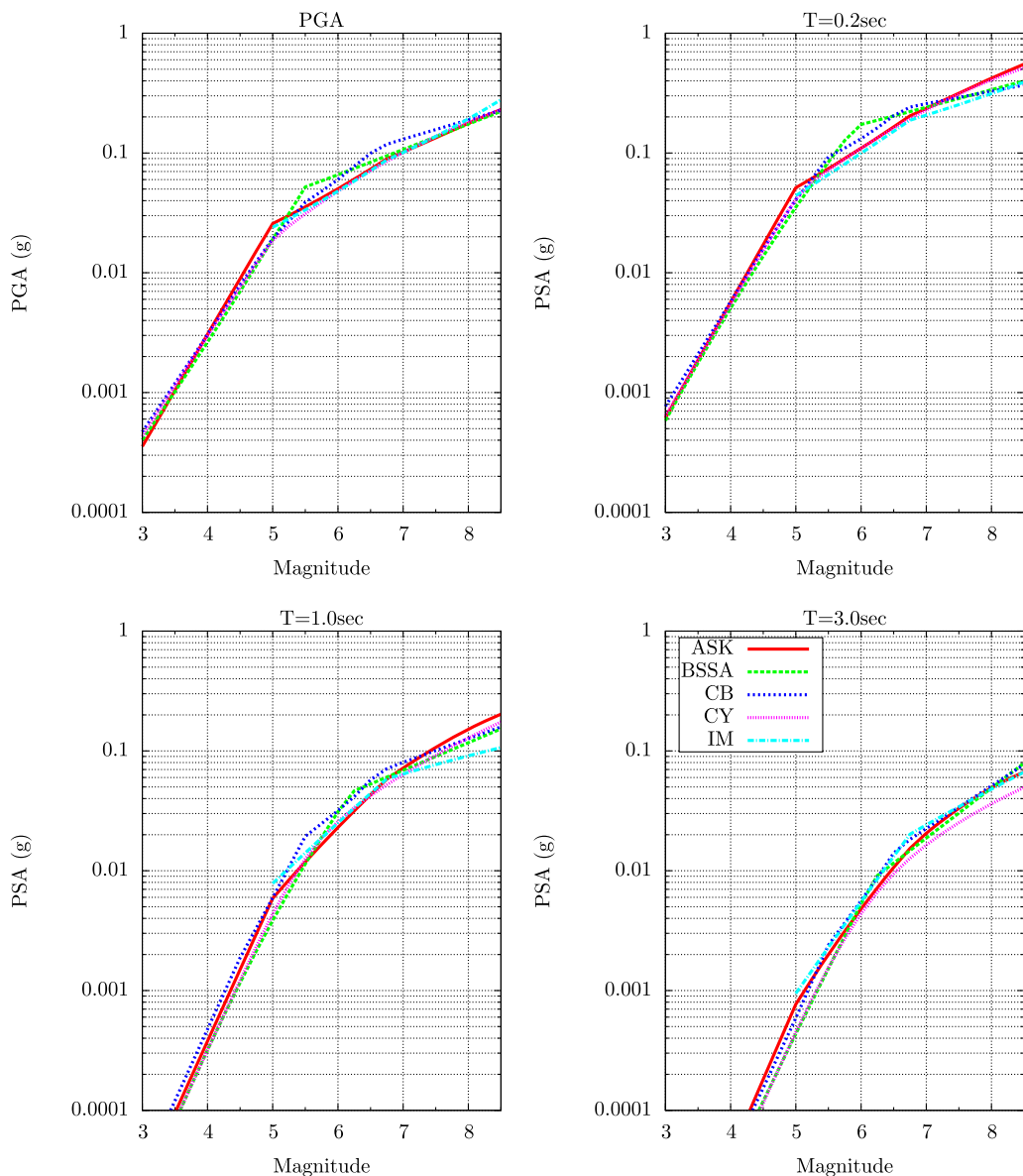
Figure 3. Comparison of magnitude scaling of the median ground motion for vertical strike-slip earthquakes at a distance of $R_{RUP} = 30$ km for $V_{S30} = 760$ m/s.

(middle) styles of faulting. The IM model does not include a hanging-wall model and is symmetric, centered about the $R_X = 0$ distance point. The BSSA model implicitly models the hanging-wall effects through the use of the R_{JB} distance metric, and locations over the fault plane have constant ground-motion values. For the ASK (using the version without the R_{Y0} feature), CB, and CY models, the hanging-wall model is part of the GMPE functional
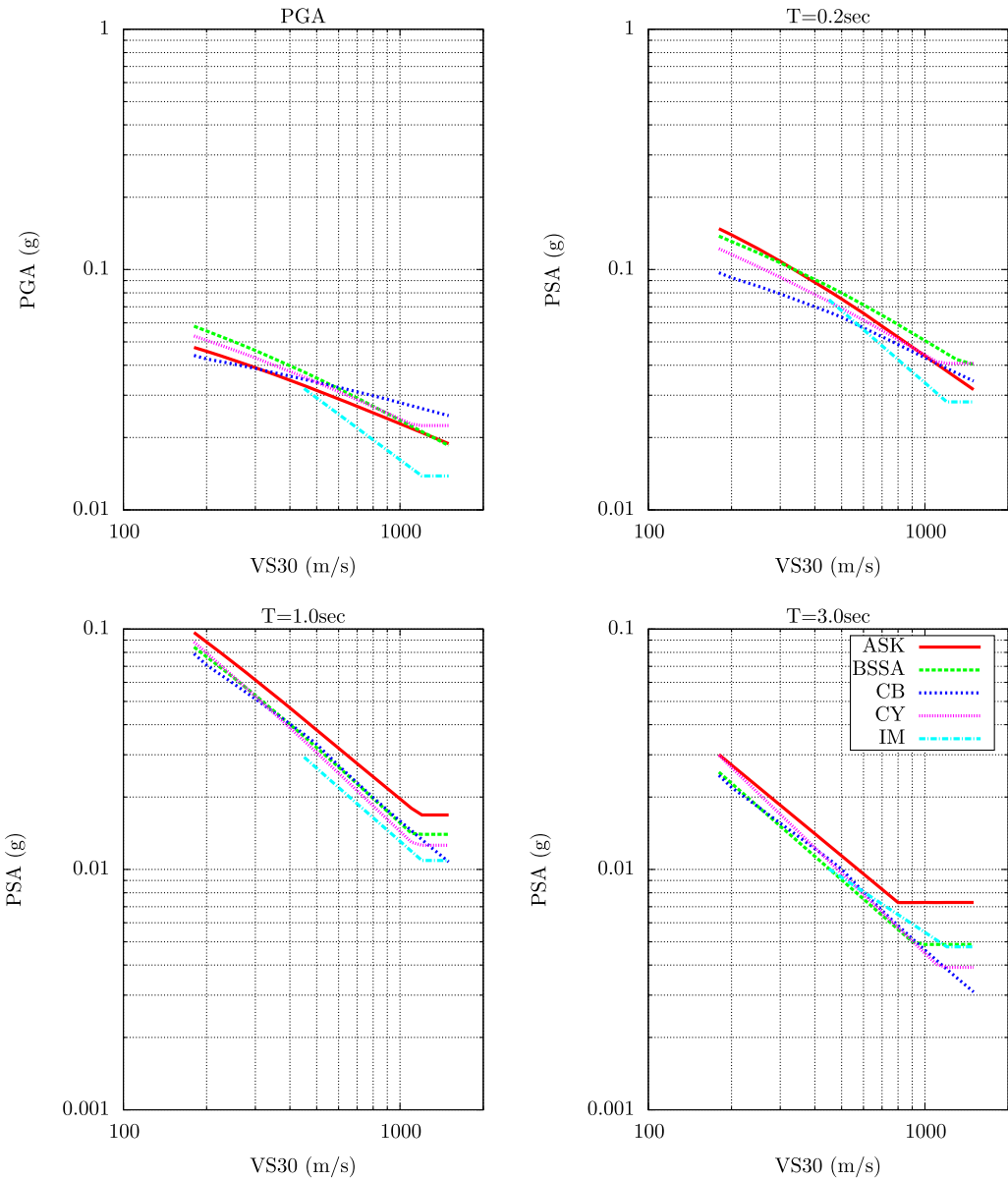
Figure 4. Comparison of V_{S30} scaling of the median ground motion for a **M** 7 strike-slip earthquake at a distance of $R_{JB} = 100$ km.

form. Overall, the differences in ground motions over the fault plane are about a factor of 2 based on the results in Figure 6, with the CB model having the strongest impact on the ground motions. This general range in ground motions is similar to what was found for the original NGA-West1 GMPEs (Abrahamson et al. 2008).
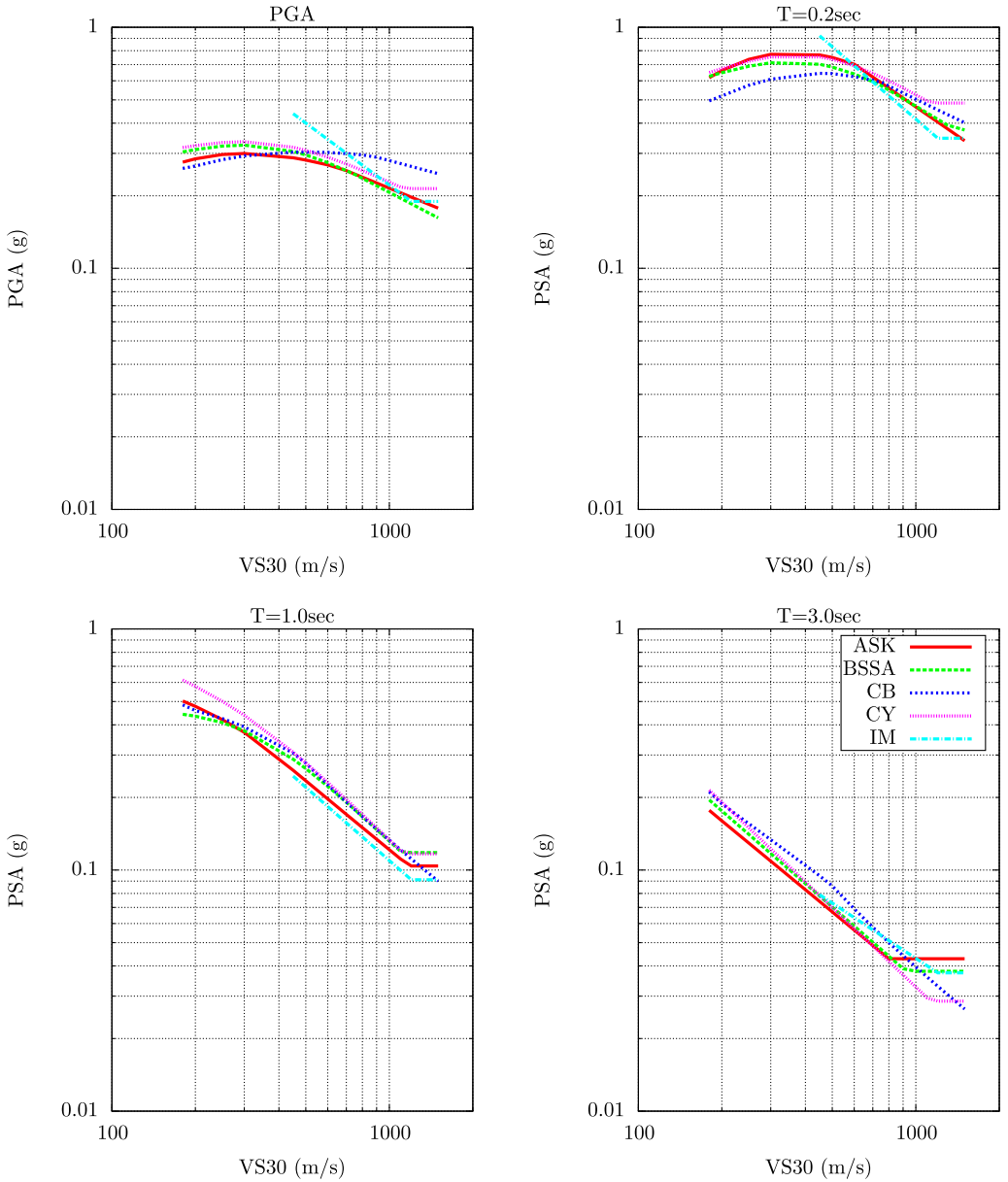
Figure 5. Comparison of V_{S30} scaling of the median ground motion for a **M** 7 strike-slip earthquake at a distance of $R_{JB} = 10$ km.

REGIONAL ADJUSTMENTS

Four of the five GMPEs (ASK, BSSA, CB, and CY) provide adjustments for different regions based on the empirical observations from the NGA-West2 database. Figure 7 shows the PGA attenuation curves ($V_{S30} = 760$ m/s) for each of these four models with their

regional adjustments for a **M**7 vertical strike-slip earthquake. As before, the depth to the top of rupture was placed at 1 km, with a hypocenter depth of 8 km. Region-specific default $Z_{1.0}$ and $Z_{2.5}$ are also provided and used with the GMPE models. Although each modeling team classified different regions, an overall conclusion can be reached that the adjustments for
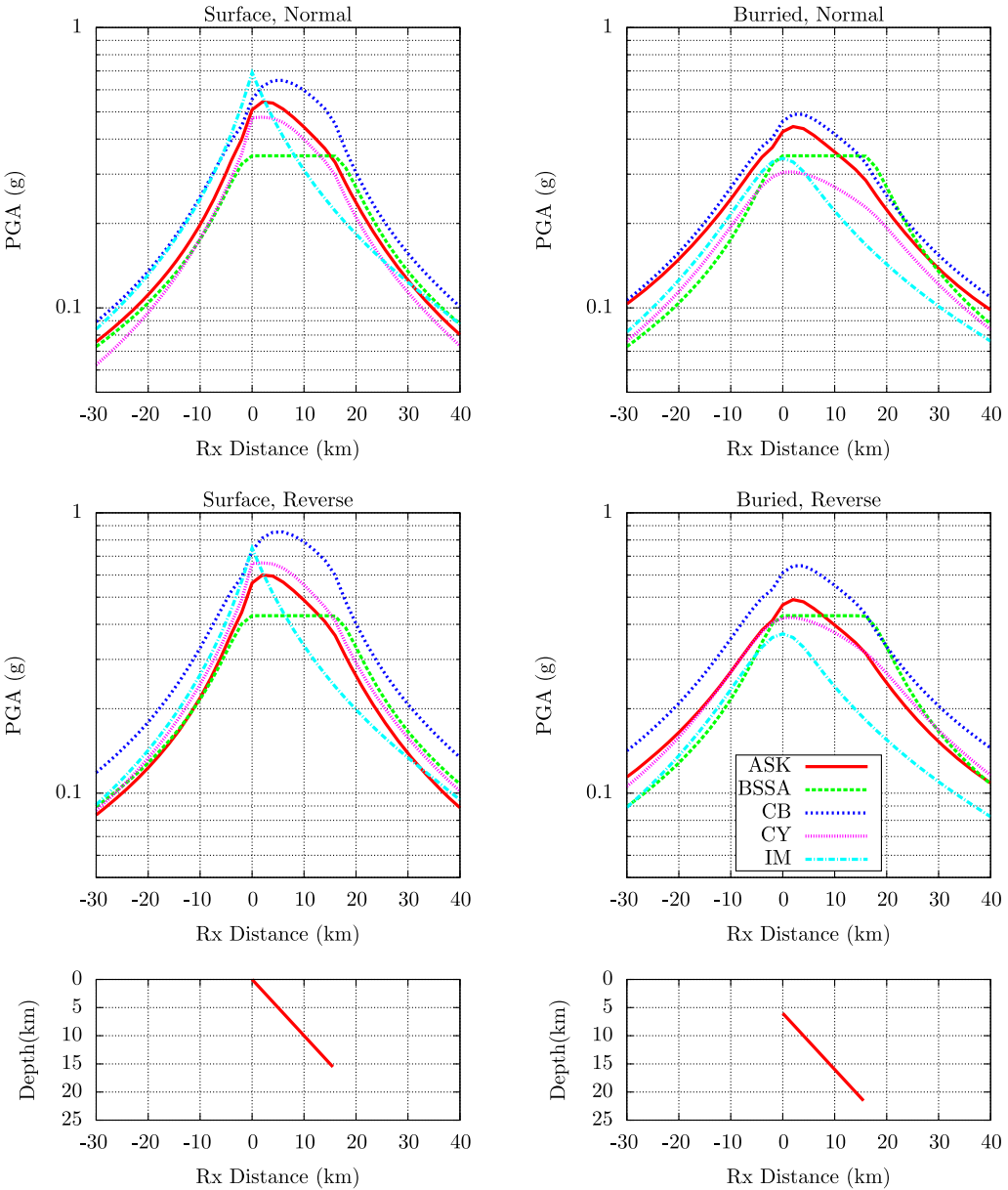
Figure 6. Comparison of FW and HW effects on PGA for a 45-degree, **M** 6.7 earthquake for $V_{S30} = 760$ m/s for both surface rupture (left side) and buried rupture (right side) with a top-of-rupture of 6 km.
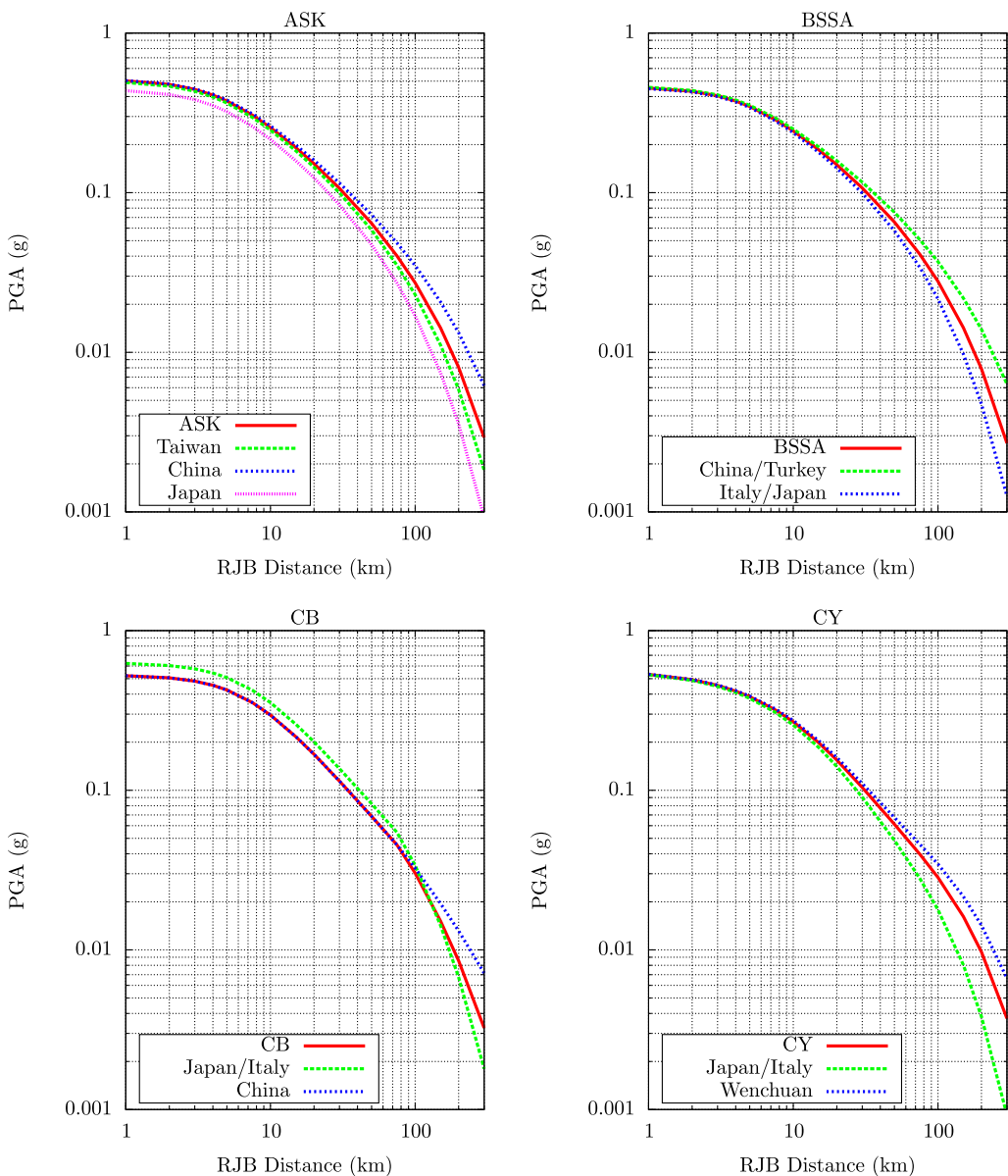
Figure 7. Comparison of regional attenuation adjustments for a **M** 7 strike-slip earthquake for PGA.

eastern China (i.e., the Wenchuan earthquake region) lead to slower attenuation with distance and that the adjustments for Italy and Japan lead to faster attenuation with distance. These adjustments, which are based on the regional data, only start to become significant for distances larger than about 80 km.

RESPONSE SPECTRA

The response spectra from **M**5, 6, 7, and 8 earthquakes for an $R_{JB} = 10$ km from a vertically dipping strike-slip fault and $V_{S30} = 760$ m/s are plotted in Figure 8. The same default parameters used in the attenuation curve comparisons (i.e., Figure 1) were used. As noted for the attenuation curves, there is similarity among the five models for the
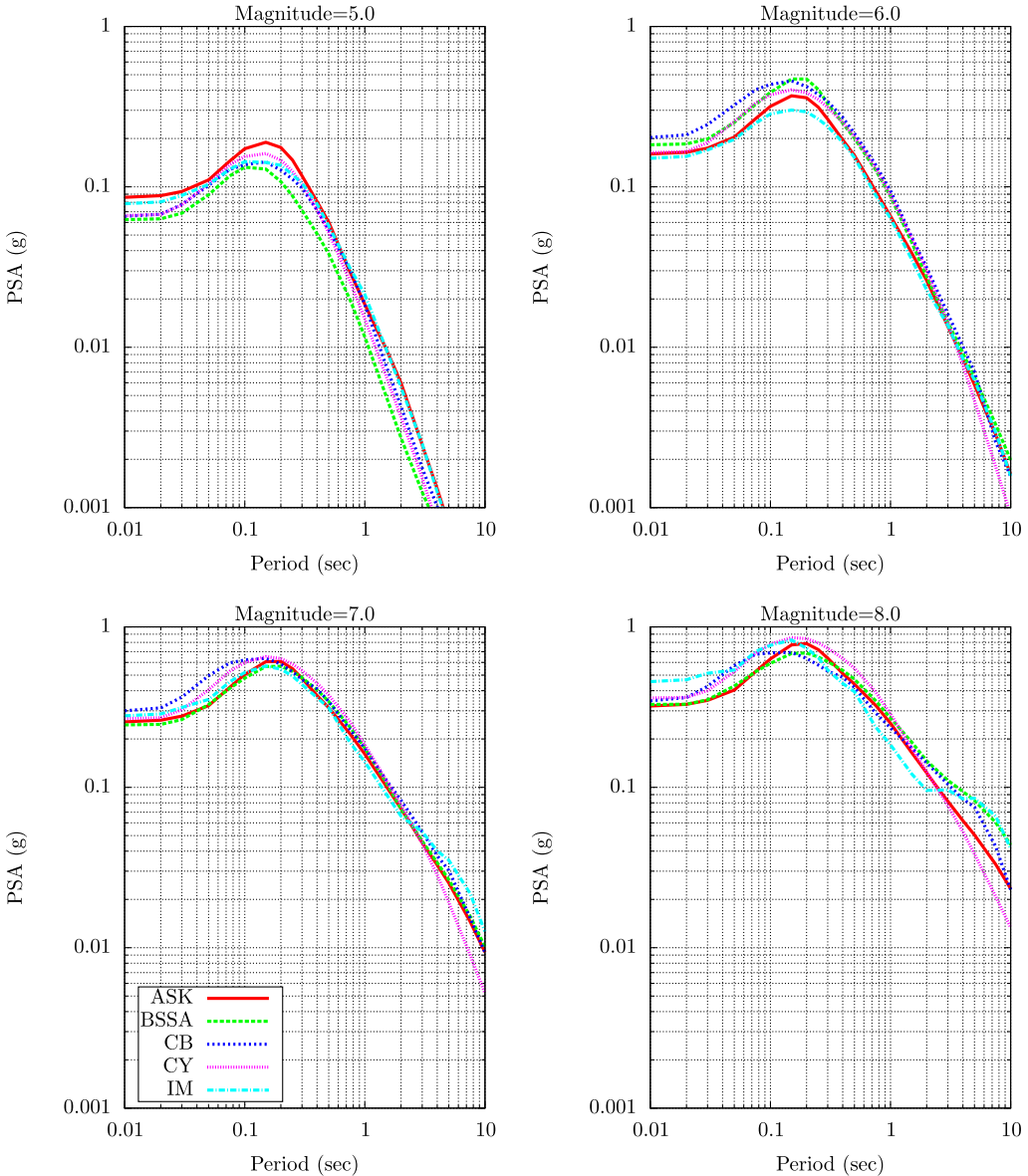
Figure 8. Comparison of median spectra for strike-slip earthquakes for $V_{S30} = 760$ m/s at an R_{JB} distance of 10 km.

M 5–7 cases. The difference between models increases for the **M**8 case, especially at the longer spectral periods.

Figure 9 compares the influence of the $Z_{1.0}$ and $Z_{2.5}$ parameters. These results are for a **M**7 vertical strike-slip earthquake at an $R_{JB} = 10$ km with a hypocenter of 8 km and top of
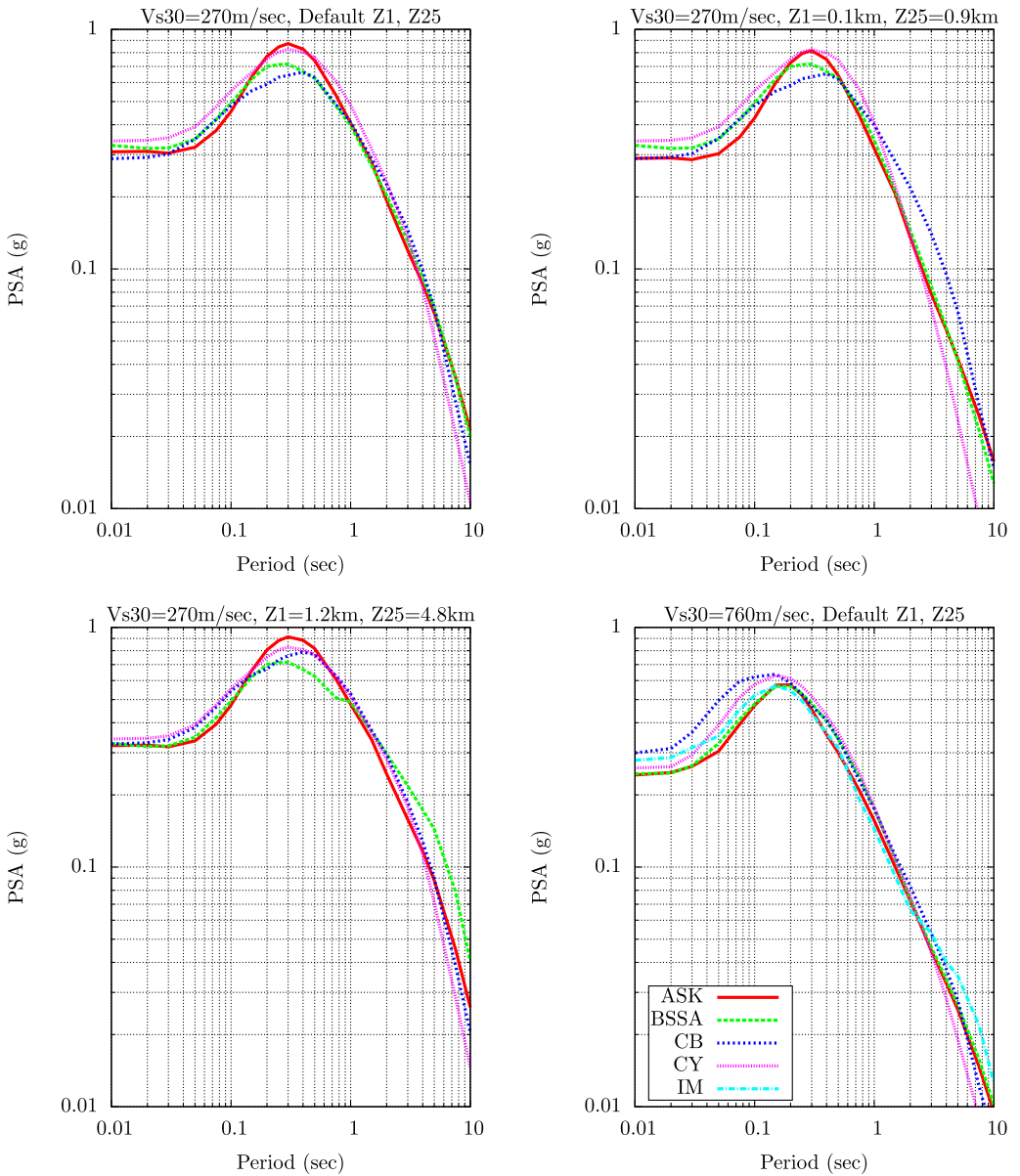

Figure 9. Comparison of median spectra for **M** 7 strike-slip earthquakes at an R_{JB} distance of 10 km with different soil depths for $V_{S30} = 270$ m/s default depth, shallow depth, deep depths, and $V_{S30} = 760$ m/s.

rupture of 1 km. The upper left spectra plot is for a $V_{S30} = 270$ m/s with the default $Z_{1.0}$ and $Z_{2.5}$ parameters. The upper right spectra plot is for a $V_{S30} = 270$ m/s with assigned $Z_{1.0} = 0.1$ km and $Z_{2.5} = 0.9$ km parameters, representing shallow basin conditions. The lower left spectra plot is for a $V_{S30} = 270$ m/s, along with $Z_{1.0} = 1.2$ km and $Z_{2.5} = 4.8$ km parameters, representing deep basin conditions. Finally, the lower right plot shows the spectra for $V_{S30} = 760$ m/s with the default depth terms for reference (see Figure 1 for default parameter values). The largest relative change in response spectra based on the different $Z_{1.0}$ and $Z_{2.5}$ values is for the longer spectral periods. For intermediate and shorter spectral periods, the range in model predictions from these non-default parameters (i.e., upper right and lower left figures) is similar to the range for the default $Z_{1.0}$ and $Z_{2.5}$ terms (i.e., upper left and lower right figures) and also the range for a $V_{S30} = 760$ m/s. However, for longer spectral periods, the observed range in the response spectra is larger for the non-default values as opposed to the default values.

COMPARISON OF THE STANDARD DEVIATIONS

The period-dependence of the aleatory variability models are compared in Figure 10 for **M**5 and 7 vertical strike-slip earthquakes at an $R_{RUP} = 30$ km and $V_{S30} = 760$ m/s. The hypocenter was fixed at 8 km for both cases, and the depth to top of rupture was 6 km and 1 km, respectively, for the **M**5 and 7 earthquakes. The total standard deviation (σ) models in general are similar, except for longer spectral periods where the IM model has a larger σ than the other four models. The **M**-dependence is shown in Figure 11 for PGA and $T = 1.0$ s
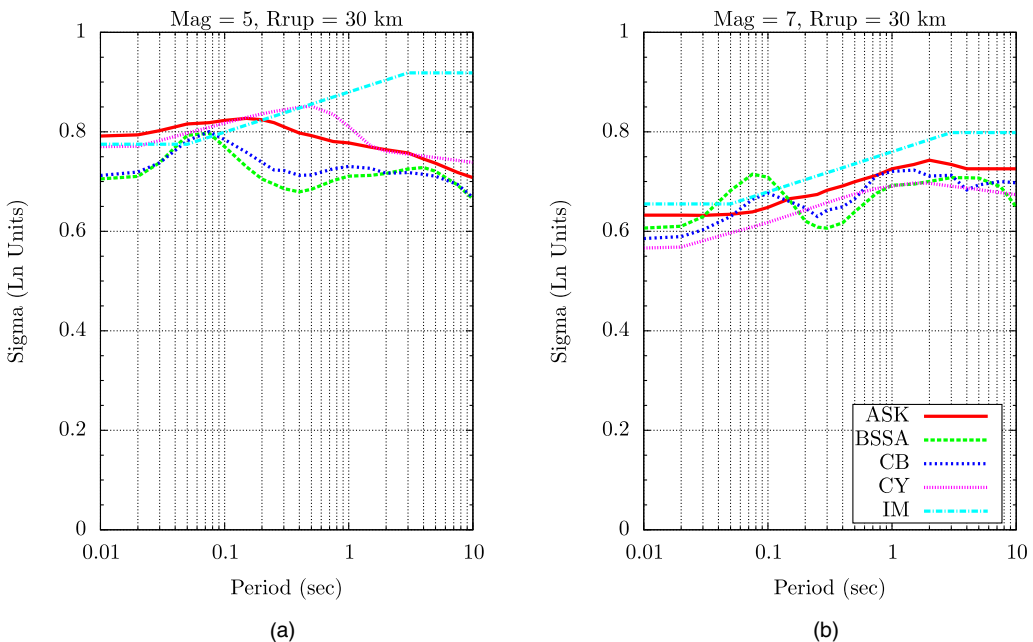

Figure 10. Comparison of the standard deviation for (a) **M** 5 and (b) **M** 7 strike-slip earthquakes at a distance of $R_{RUP} = 30$ km for $V_{S30} = 760$ m/s.
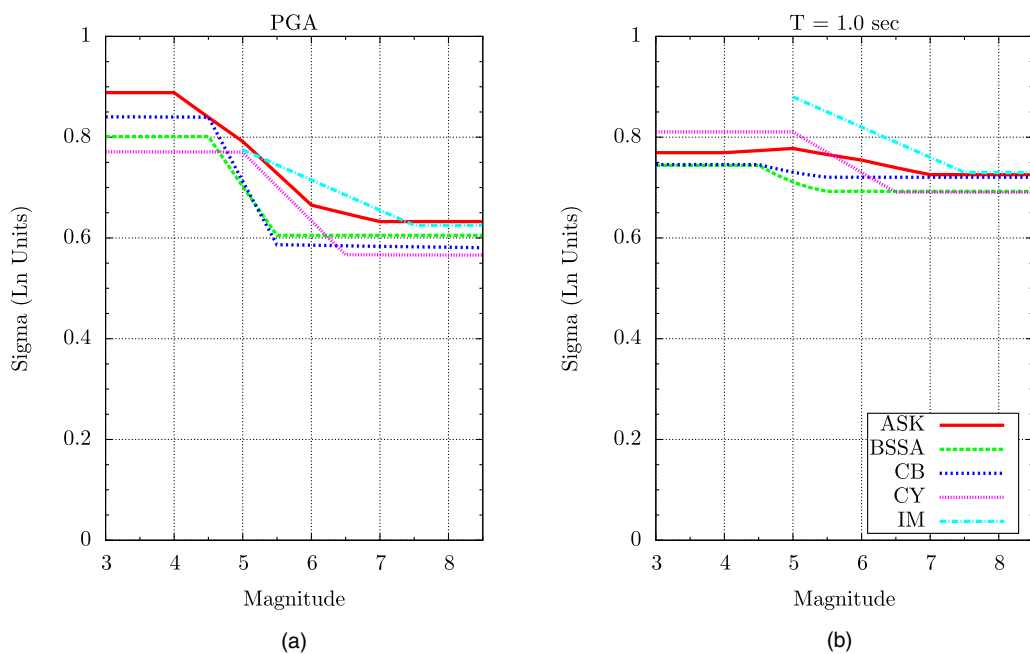
Figure 11. Comparison of magnitude dependence of the standard deviation for (a) PGA and (b) $T = 10$ s for strike-slip earthquakes at a distance of $R_{RUP} = 30$ km for $V_{S30} = 760$ m/s.
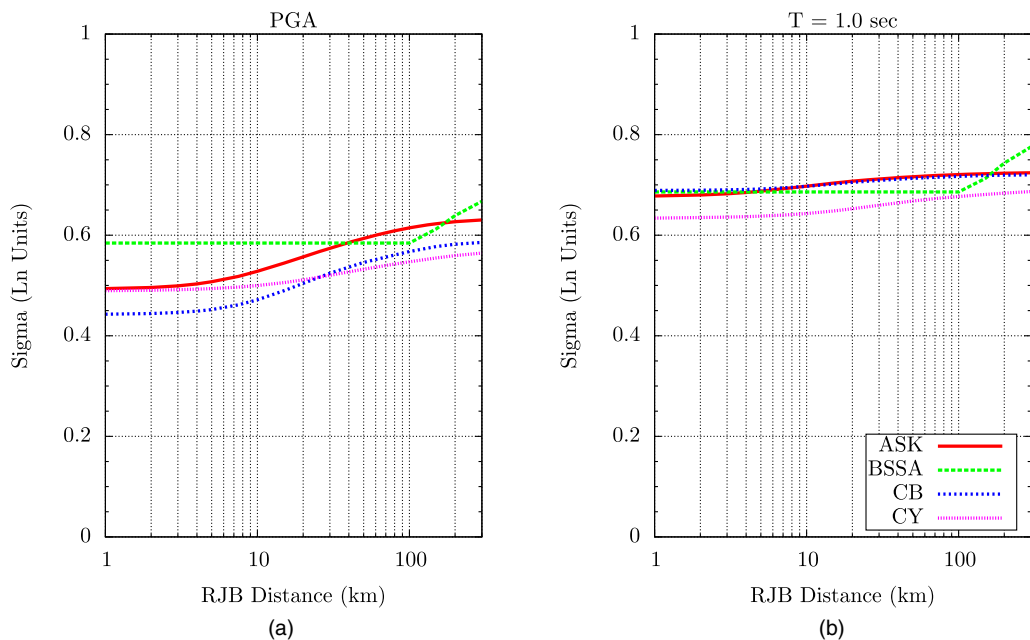

Figure 12. Comparison of the standard deviation for (a) PGA and (b) $T = 10$ s for a **M** 7 strike-slip earthquake and $V_{S30} = 270$ m/s.

PSA for $V_{S30} = 760$ m/s at a R_{RUP} distance of 30 km; the PGA results have a stronger magnitude-dependence than the $T = 1.0$ s PSA results, with higher values of σ for the smaller-magnitude events. Finally, a comparison of σ for a **M**7 vertical strike-slip earthquake as a function of R_{JB} for PGA and $T = 1.0$ s PSA is shown in Figure 12 for $V_{S30} = 270$ m/s. For both PGA and $T = 1.0$ s PSA, the sigma values increase with increasing R_{JB} distance.

CONCLUSIONS

Overall, the suite of five NGA GMPEs was found to provide median ground-motion predictions that agree to within factors of about 1.5–2. The largest differences are observed for the cases in which the NGA-West2 database is sparse, such as for large (**M**8) earthquakes at close distances, and for hanging-wall sites located over the rupture plane of shallow-dipping earthquakes. Consistent regional attenuation adjustments are provided for four of the GMPEs, based on the analysis of the regional data sets contained within the NGA-West2 data set. All aleatory variability models are magnitude- and distance-dependent, with larger total standard deviation values for the smaller earthquake magnitudes and larger distances.

ACKNOWLEDGMENTS

REFERENCES

Abrahamson, N. A., Silva, W. J., and Kamai, R., 2014. Summary of the ASK14 ground motion relation for active crustal regions, *Earthquake Spectra* **30**, 1025–1055.

Abrahamson, N. A., Atkinson, G. M., Boore, D., Bozorgnia, Y., Campbell, K., Chiou, B. S.-J., Idriss, I. M., Silva, W., and Youngs, R., 2008. Comparisons of the NGA ground-motion relations, *Earthquake Spectra*, **24**, 45–66.

Ancheta, T. D., Darragh, R. B., Stewart, J. P., Seyhan, E., Silva, W. J., Chiou, B. S.-J., Wooddell, K. E., Graves, R. W., Kottke, A. R., Boore, D. M., Kishida, T., and Donahue, J. L., 2014. NGA-West2 database, *Earthquake Spectra* **30**, 989–1005.

Atkinson, G. M., and Boore, D. M., 2011. Modifications to existing ground-motion prediction equations in light of new data, *Bull. Seismol. Soc. Am.* **101**, 1121–1135.

Boore, D. M., Stewart, J. P., Seyhan, E., and Atkinson, G. M., 2014. NGA-West2 equations for predicting PGA, PGV, and 5% damped PSA for shallow crustal earthquakes, *Earthquake Spectra* **30**, 1057–1085.

Bozorgnia, Y., Abrahamson, N. A., Al Atik, L., Ancheta, T. D., Atkinson, G. M., Baker, J. W., Baltay, A., Boore, D. M., Campbell, K. W., Chiou, B. S.-J., Darragh, R., Day, S., Donahue, J., Graves, R. W., Gregor, N., Hanks, T., Idriss, I. M., Kamai, R., Kishida, T., Kottke, A., Mahin, S. A., Rezaeian, S., Rowshandel, B., Seyhan, E., Shahi, S., Shantz, T., Silva, W., Spudich, P., Stewart, J. P., Watson-Lamprey, J., Wooddell, K., and Youngs, R., 2014. NGA-West2 research project, *Earthquake Spectra* **30**, 973–987.

Campbell, K. W., and Bozorgnia, Y., 2014. NGA-West2 ground motion model for the average horizontal components of PGA, PGV, and 5% damped linear acceleration response spectra, *Earthquake Spectra* **30**, 1087–1115.

Campbell, K. W., 2011. Ground motion simulation using the hybrid empirical method: Issues and insights, in *Earthquake Data in Engineering Seismology*, S. Akkar, P. Gülkan, and T. van Eck (editors.), Geotechnical, Geological, and Earthquake Engineering 14, Chapter 7, Springer, Berlin, 81–95.

Chiou, B. S.-J., and Youngs, R. R., 2014. Update of the Chiou and Youngs NGA model for the average horizontal component of peak ground motion and response spectra, *Earthquake Spectra* **30**, 1117–1153.

Chiou, B. S.-J., Youngs, R. R., Abrahamson, N. A., and Addo, K., 2010. Ground motion attenuation model for small to moderate shallow crustal earthquakes in California and its implications on regionalization of ground motion prediction equations, *Earthquake Spectra* **26**, 907–926.

Idriss, I. M., 2014. An NGA-West2 empirical model for estimating the horizontal spectral values generated by shallow crustal earthquakes, *Earthquake Spectra* **30**, 1155–1177.

Kamai, R., Abrahamson, N. A., and Silva, W. J., 2014. Nonlinear horizontal site amplification for constraining the NGA-West2 GMPEs, *Earthquake Spectra* **30**, 1223–1240.

Powers, M., Chiou, B. S.-J., Abrahamson, N. A., Bozorgnia, Y., Shantz, T., and Roblee, C., 2008. An overview of the NGA project, *Earthquake Spectra* **24**, 3–22.

Seyhan, E., Stewart, J. P., Ancheta, T. D., Darragh, R. B., and Graves, R. W., 2014. NGA-West2 site database, *Earthquake Spectra* **30**, 1007–1024.

Seyhan, E., and Stewart, J. P., 2014. Semi-empirical nonlinear site amplification from NGA-West2 data and simulations, *Earthquake Spectra* **30**, 1241–1256.

Walling, M., Silva, W. J., and Abrahamson, N. A., 2008. Non-linear site amplification factors for constraining the NGA models, *Earthquake Spectra* **24**, 243–255.

Wooddell, K. E., and Abrahamson, N. A., 2014. Classification of main shocks and aftershocks in the NGA-West2 database, *Earthquake Spectra* **30**, 1257–1267.